Correlation between Phase Behavior and Tensile Properties of Diblock Copolymers

R. Weidisch,*,† M. Stamm,† D. W. Schubert,‡ M. Arnold,§ H. Budde,§ and S. Höring§

Max-Planck-Institut für Polymerforschung, Postfach 3148, 55021 Mainz, Germany; GKSS Forschungszentrum, Max-Planck-Strasse, 21502 Geesthacht, Germany; and Martin-Luther-Universität Halle-Wittenberg, Institut für Technische und Makromolekulare Chemie, 06108 Halle/Saale, Germany

Received November 10, 1998; Revised Manuscript Received March 2, 1999

ABSTRACT: The phase behavior of poly(styrene-*b*-butyl methacrylate), PS-*b*-PBMA, diblock copolymers was investigated by small-angle neutron scattering (SANS), neutron reflectometry (NR), and rheology. For a symmetrical P(dS-*b*-nBMA) diblock copolymer a lower critical order transition (LCOT) at 155 °C was found by SANS and rheology. Furthermore, the temperature-dependent interaction parameter was determined in the temperature regime between 110 and 145 °C from fits to the scattering curves in the disordered region. The interaction parameter increases with increasing temperature and shows a weak temperature dependence. The LCOT behavior thus is expected to be a large entropic contribution to χ. The interfacial width observed by NR is relatively large compared to other diblock copolymers. Different block copolymers were investigated with respect to the influence of miscibility on tensile properties. While poly(styrene-*b*-butyl methacrylate) diblock copolymers show significant synergistic effects on tensile properties, for poly(methyl methacrylate-*b*-butyl methacrylate) diblock copolymers no significant synergistic effects on tensile properties were observed due to the increased interaction parameter and the smaller interfacial width as compared to the case of PS-*b*-PBMA diblock copolymers.

Introduction

Block copolymers usually show a macroscopical grain structure at a size scale of 1−10 μm as well as structures in the nanometers scale. Such materials will exhibit isotropic properties in the case of the absence of macroscopic orientations. Therefore, block copolymers show a high transparency which leads to interesting applications.[1−2] In poly(styrene-*b*-isoprene) (PS-*b*-PI) diblock copolymers the following morphologies were reported: BCC spheres, hexagonally packed cylinders, ordered bicontinuous double diamond (OBDD), and lamellar structures.[3−6] In the weak segregation limit the perforated layers and the cubic bicontinuous structure ("gyroid") were found in addition.[7−9] It was shown for several block copolymer systems that an order−disorder transition can be observed where the microstructures will be destroyed, and an isotropic homogeneous phase is formed. In contrast to most other block copolymers, PS-*b*-PBMA diblock copolymers show, however, a lower critical order transition (LCOT).[10,11] SAXS experiments have shown the existence of both an upper critical order transition (UCOT) and a lower critical order transition (LCOT). Ruzette et al.[38] have shown that dPS-*b*-alkyl methacrylate diblock copolymers with long side chain methacrylates ($n \geq 6$) reveal an UCOT behavior. In contrast, diblock copolymers with short side chain methacrylates ($n < 5$) reveal a LCOT behavior. Furthermore, recently Russell[12] and co-workers have reported that an increase of pressure drives the system into the disordered state. The correlation between the Flory−Huggins interaction parameter and the interface width between polymers has been a subject of many studies.[13−16] It is now interesting to determine the temperature dependence of the interaction parameter for an LCOT system where the entropic contribution should be quite large. From this we might be able to get a deeper understanding of the phase behavior of PS-*b*-PBMA diblock copolymers and their correlation with tensile properties.

In previous investigations by dynamic mechanical analysis (DMA) PS-*b*-PBMA reveals a weak segregation at higher molecular weights. This method allows us to investigate the correlation between phase behavior and mechanical properties in the molecular weight range of $M_n > 200$ kg/mol[17−19] since the mechanical properties do not show a molecular weight dependence. The phase behavior and interface formation were found to be important for the mechanical properties of polymer blends, and the low interfacial adhesion between immiscible polymer pairs is believed to be the reason for their low toughness. For block copolymers this correlation was not reported in the literature but is also quite important. To describe the influence of miscibility and interface formation on tensile properties of block copolymers, we compare the results for PS-*b*-PBMA diblock copolymer with PMMA-*b*-PBMA diblock copolymers where the interaction parameter is much larger.

Experimental Section

Polymerization Procedure. All polymerizations were carried out in carefully flamed glass reactors in THF as the solvent at −78 °C under argon atmosphere using syringe techniques. After several cycles of degassing the monomer over calcium hydride, the monomer was introduced into the reactor by condensation under reduced pressure. Then the desired amount of initiator was added at once, and after 15 min the living polystyrene or methyl methacrylate anions were end-capped with diphenylethylene. Butyl methacrylate as the second monomer was added dropwise very slowly with a syringe. The living anions were terminated by adding methanol after another 30 min. Then, the polymer was precipitated in a 7/3 methanol/water mixture at −30 °C, washed, and dried

† Max-Planck-Institut für Polymerforschung.
‡ GKSS Forschungszentrum.
§ Martin-Luther-Universität Halle-Wittenberg.
* Corresponding author.

10.1021/ma981748t CCC: $18.00
Published on Web 04/21/1999

Table 1. Molecular Weight (M_n), Volume Fraction (Φ_{PS}), and Polydispersity (M_w/M_n) for DPS-*b*-PBMA Diblock Copolymers Used in This Study

sample	$10^{-3}M_n$[a] copolymer (M_w/M_n)	Φ_{PS}[b] block
SBM90	90.0 (1.06)	0.55
SBM150	148.8 (1.07)	0.50
SBM250	248.3 (1.05)	0.51

[a] Size exclusion chromatography (SEC), values are based on the PS standards. [b] ^{1}H NMR.

in a vacuum for several days. With some materials the polystyrene block was deuterated to achieve a contrast for neutron scattering. The deuterated samples are denoted by dPS-*b*-PnBMA or dPMMA-*b*-PBMA. The deuteration is achieved by using deuterated styrene in the synthesis of the copolymers. The sample characteristics are given in Table 1.

Sample Preparation. All samples were dissolved in toluene. The solvent was allowed to evaporate slowly over 5−7 days at room temperature. Then the films were dried to constant weight in a vacuum oven at 120 °C for 3 days. For SANS experiments melt pressed (T = 140 °C) samples as well as films as described before were used. An annealing temperature of 140 °C was used for the PMMA-*b*-PBMA block copolymers because of the higher T_g of the PMMA block. This allowed to achieve nearly equilibrium morphologies for these block copolymers.

Measurements. Measurements with size exclusion chromatography (SEC) were carried out on a Knauer-SEC with a RI/viscodetector and a PS standard column. The volume fractions of the diblock copolymers were estimated by ^{1}H NMR. Neutron reflectometry (NR) experiments were performed at the neutron reflectometer TOREMA II at GKSS Research Centre, Geesthacht. The wavelength is fixed to λ = 0.43 nm, and a position sensitive gas detector is used. Samples were prepared by spin coating[20] on 10 × 10 cm^2 float glass plates as a substrate and have been annealed at different temperatures for 2 weeks. They are quenched to room temperature for the NR experiments. Small-angle neutron scattering (SANS) measurements were performed at the small-angle scattering facility KWS II located at GKSS Geesthacht. All used samples were melt-pressed into 1 mm thick and 13 mm diameter disks. The instrument configuration was λ = 0.91 nm and $\Delta\lambda/\lambda$ = 0.2 due to the velocity selector and sample−detector distance of 5.6 m. The scattering data were corrected for detector sensitivity, background scattering, used sample thickness, and transmission and placed on an absolute basis using several standards. The SANS profiles at different temperatures are discussed as a function of the scattering vector $q = (4\pi/\lambda)\sin(\theta)$, where 2θ is the scattering angle. The dynamic storage and loss shear moduli, G' and G'', were determined with a Rheometrics RMS 800 using the temperature step mode and a frequency of 0.01 rad/s and a amplidude of 5%. Tensile tests were performed on a universal testing machine (Zwick 1425) at a strain rate of 1.6 × 10^{-4} s^{-1}. The tensile bars had a thickness of 0.5 mm and a total length of 50 mm. For each measured data point at least 10 samples were investigated.

Phase Behavior and Interface Formation of dPS-*b*-PBMA Diblock Copolymers

The phase behavior of PS-*b*-PBMA diblock copolymers was investigated by SANS, NR, and DMA. SANS experiments were performed at temperatures in the range 110−180 °C. Before starting the experiment, the samples were annealed for 2 days at 110 °C in order to achieve equilibrium. In Figure 1 the scattering profiles for a dPS-*b*-PnBMA diblock copolymer with 90 kg/mol and 55 vol % PS (sample SBM90 in Table 1) are shown as a function of temperature. At low temperature the sample exhibits a diffuse scattering maximum with a wide full width at half-maximum, Δq. With increasing temperatures the peak intensifies, increases, and sharpens which lead to the conclusion that the copolymer is approaching a ordering transition with increasing temperature (LCOT) as described by Russell and co-workers.[10] Figure 2 shows the peak position q^*, the peak intensity $I(q^*)$, and the full width at half-maximum (fhwm) Δq as a function of temperature as determined by a Lorentzian fit. The peak intensity is strongly increased at 155 °C, and accordingly the value of Δq strongly decreased, indicating a disorder−order transition (LCOT) at this temperature. The value of q^* decreases with increasing temperature, indicating a stretched chain conformation at higher temperatures due to the transition to the ordered state. In contrast to the dependence of $I(q^*)$ and Δq, q^* displays no strong discontinuity. For poly(ethylene-*b*-ethylenepropylene) block copolymers different dependencies of ln q^* on temperature above and below the order−disorder tran-

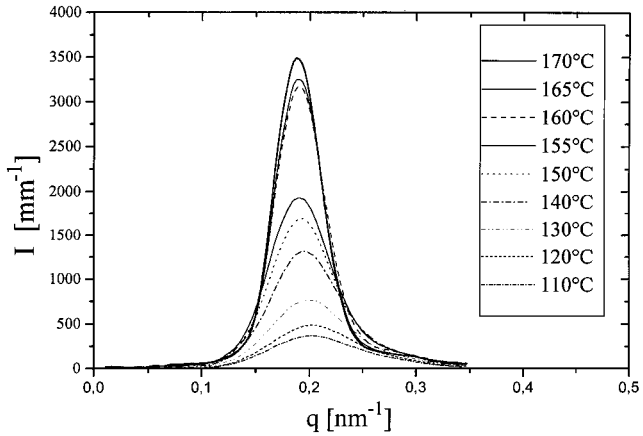

Figure 1. Small-angle neutron scattering (SANS) profiles for a dPS-*b*-PnBMA diblock copolymer with M_n = 90 kg/mol and 55% PS at different temperatures.

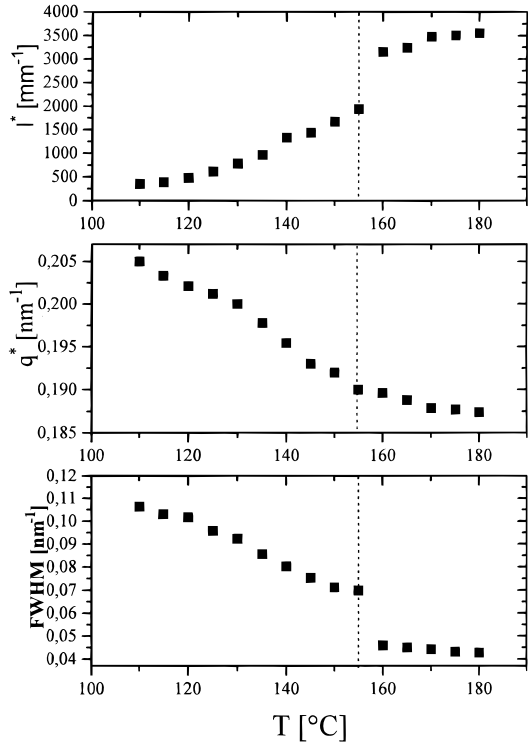

Figure 2. Dependence of intensity at maximum position $I(q^*)$, peak position of scattering vector q^*, and the full width at half-maximum fwhm (Δq) on temperature for a dPS-*b*-PnBMA diblock copolymer with M_n = 90 kg/mol and 55% PS.

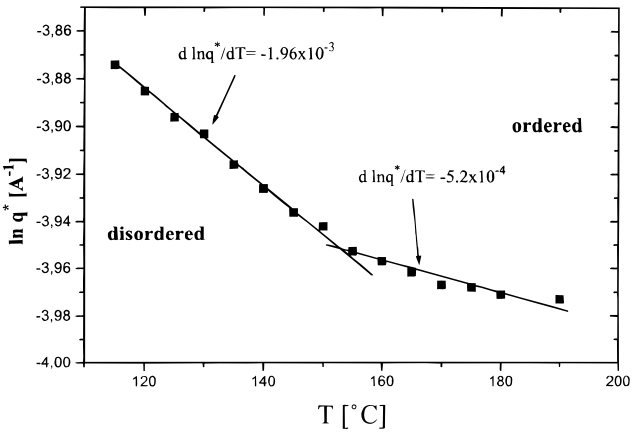

Figure 3. Temperature dependence of peak position q^* for a dPS-*b*-PnBMA diblock copolymer with M_n = 90 kg/mol and 55% PS.

sition were observed.[21] As shown in Figure 3 also for PS-*b*-PBMA diblock copolymers such dependencies can be found: $\partial \ln q^*/\partial T \approx -1.96 \times 10^{-3}$ below approximately 140 °C and $\partial \ln q^*/\partial T \approx -5.2 \times 10^{-4}$ above 160 °C. Comparing these regimes with the dependencies of $I(q^*)$ and Δq, it is found that the change in the slope of $\partial \ln q^*/\partial T$ at 155 °C corresponds to the T_{DOT} as obtained from the jump in $I(q^*)$ and Δq. This means that all data $I(q^*)$, Δq, and q^* indicate a disorder−order transition at 155 °C. The same transition temperature was found in rheology indicated by the strong increase of the storage modulus at 155 °C (Figure 4). As the DOT is approached, the composition profile becomes increasingly sinusoidal, and the softening of the ordered state permits the stretched coils into their unperturbed conformation which corresponds to the change of $\partial \ln q^*/\partial T$.[22] This is also visible for our system where the largest value of $\partial \ln q^*/\partial T$ can be observed in the disordered state below 155 °C. Assuming incompressibility, the scattering intensity $I(q)$ in the disordered state is given by the theory of Leibler:[23]

$$I(q) = (b_A - b_B)v^{-1}S(q) \tag{1}$$

The structure factor $S(q)$ is defined as

$$S(q) = \frac{1}{F(q) - 2\chi} \tag{2}$$

$$x = q^2 R_g{}^2 = \frac{q^2 N a^2}{6} \tag{3}$$

$$F(x,\varphi) = \frac{g_1(1,x)}{\{g_1(\varphi,x)\, g_1(1-\varphi,x) - [g_1(1,x) - g_1(\varphi,x) - g_1(1-\varphi,x)]^2/4\}} \tag{4}$$

$$g_1(\varphi,x) = \frac{2}{x^2}[\exp(-\varphi x) - 1 + \varphi x] \quad \text{(Debye function)} \tag{5}$$

where b_A and b_B are the segment scattering lengths, v is the mean segment volume, R_G is the radius of gyration, and $F(x,f)$ is the correlation function for a melt of Gaussian diblock copolymer coils.

For temperatures between 110 and 145 °C the calculation works well where the inverse peak intensity varied linearly with the inverse temperature. A representative Leibler fit is shown in Figure 5 for a scattering profile at 120 °C. It is evident from Figure 5 that the agreement between the Leibler fit and the scattering curve is very good over the entire scattering vector range. The experimental points at very small q ($q < 0.01$ nm^{-1}) are slightly larger than in the fit. This disagreement could be due to the finite compressibility of the copolymer melt not taken into account in the theory. The temperature dependence of χ can be described as a sum of terms of entropic and enthalpic contributions χ_S and χ_H. From the calculated scattering profiles the temperature dependence of χ was obtained (Figure 6), which can be described by

$$\chi = (0.0243 \pm 0.0004) - \frac{4.56 \pm 0.169}{T} \tag{6}$$

χ increases with increasing temperatures, indicating a LCOT behavior. The temperature dependence of χ is quite small compared to that of other block copolymers. It is obtained from eq 6 that the entropic contribution to χ (first term in eq 6) is relatively large compared to that of the enthalpic contribution (second term in eq 6). For PS-*b*-PMMA and PS-*b*-alkyl methacrylate diblock copolymers with long side chain methacrylates ($n \geq 6$) the entropic and enthalpic contributions are comparable in size with our system. However, this system shows an UCOT behavior.[24,38] It should be mentioned that χ could be only determined in the temperature regime between 110 and 145 °C. Higher temperatures were

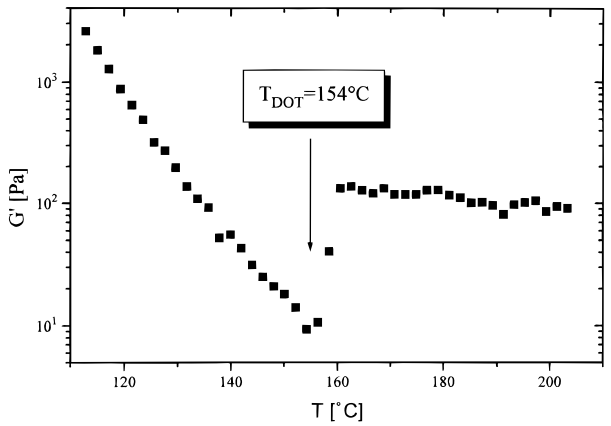

Figure 4. Dependence of storage modulus G' on temperature for a dPS-*b*-PnBMA diblock copolymer with M_n = 90 kg/mol and 55% PS measured at a frequency of 0.01 rad/s.

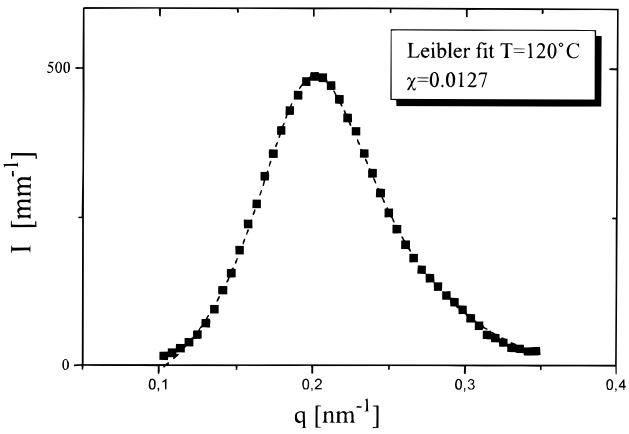

Figure 5. Comparison of the calculated and experimental neutron scattering profiles at T = 120 °C for a dPS-*b*-PnBMA diblock copolymer with M_n = 90 kg/mol and 55% PS.

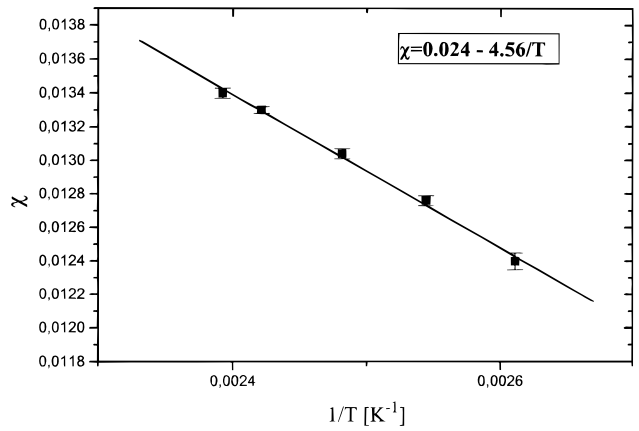

Figure 6. Interaction parameter χ as a function of reciprocal temperature for a dPS-*b*-PnBMA diblock copolymer with M_n = 90 kg/mol and 55% PS.

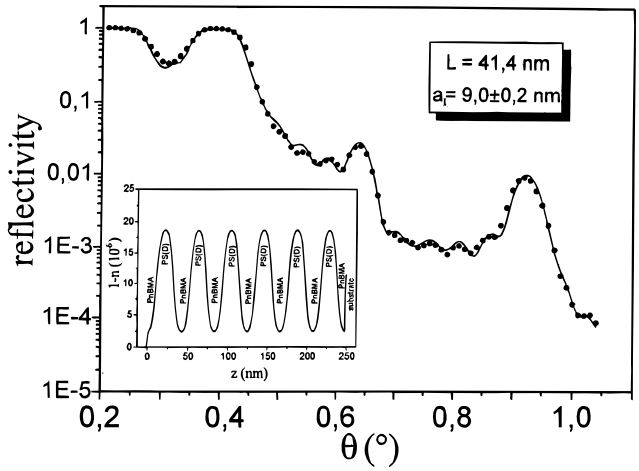

Figure 7. Neutron reflectivity data (●) and calculated fit curve from a thin film of a dPS-*b*-nBMA diblock copolymer with M_n = 148 kg/mol and 50% PS. The inset shows the corresponding refractive index profile normal to the film surface that was used to calculate the reflectivity.

limited by the transition to the ordered state and lower temperatures by the glass transition of PS, which it makes difficult to achieve equilibrium. For a symmetical diblock copolymer, the order−disorder transition is predicted by Leibler[23] for $(\chi N)_{ODT} = 10.495$. More recent theories include fluctuation effects which lead to an correction of the theory in order of $N^{-1/3}$.[25] For a PS-*b*-PBMA diblock copolymer with 90 kg/mol and 55% PS the value of χN increases from 9.43 at 110 °C up to 10.19 at 145 °C. At 155 °C, where the disorder−order transition occurs, the value of χN turns out to be 10.38, which is in good agreement with the predicted value from Leibler within experimental error and calculated fits. The ordered state is reached at 160 °C as indicated by rheology and SANS where $\chi N = 10.48$.

For the NR experiments two symmetric diblock copolymers of dPS and PnBMA were used ($\varphi \approx 0.5$, sample SBM250: M_n = 248 300 g/mol and sample SBM150: M_n = 148 800 g/mol, respectively), where the polystyrene block was deuterated for contrast reasons. The temperature dependence of the long period and interfacial width obtained in NR experiments can be understood with a temperature-dependent interaction parameter χ as already determined from SANS as discussed before. We use a mean segment length b = 0.78 nm. The analysis of specular reflectivity curves

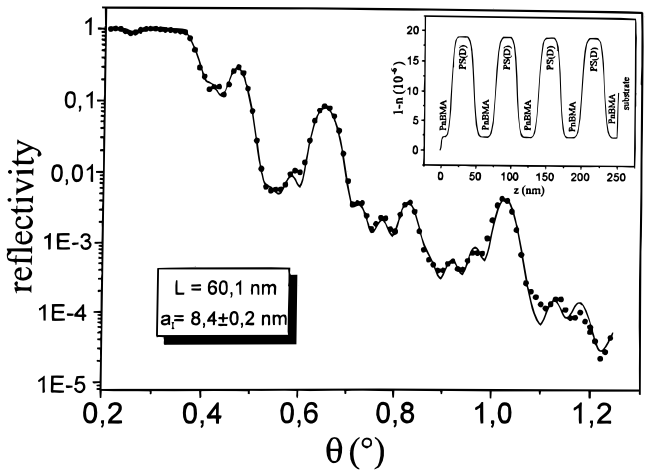

Figure 8. Neutron reflectivity data (●) and calculated fit curve from a thin film of a dPS-*b*-nBMA diblock copolymer with M_n = 248 kg/mol and 51% PS. The inset shows the corresponding refractive index profile normal to the film surface that was used to calculate the reflectivity.

(Figures 7 and 8) yields information on the neutron refractive index and composition profile perpendicular to the interface.[26] The lamella are highly oriented parallel to the substrate, and the profile details are obtained from NR, averaged laterally over the coherence length of the neutrons. The interfacial profile between microphase separated regions is described by a hyperbolic tangent profile, which is a trivial profile assumed in theoretical approximations.[27] However, the hyperbolic tangent profile is exact for the interface between strong incompatible homopolymers.[16,26]

The theory by Semenov[25] predicts for the lamellar morphology of symmetric diblock copolymers the period L and interfacial width a_I in the strong segregation limit.

$$L = 4\left(\frac{3}{\pi^2}\right)^{1/3}\frac{b}{\sqrt{6}}N^{2/3}\chi^{1/6} \tag{7}$$

$$a_I = \frac{2b}{\sqrt{6\chi}}\left[1 + \frac{1.34}{(\chi N)^{1/3}}\right] + \text{fluctuation corrections} \tag{8}$$

Calculating the period L from eq 7 based on the χ values determined by SANS, one finds an good agreement with the NR results. Regarding the interfacial width a_I, the experimentally determined values of 9.0 nm for sample SBM150 and 8.4 nm for sample SBM250 are slightly larger than predicted from eq 8. The deviation might be due to the fact that eq 8 was derived in the strong segregation limit, and for the present case χN is 16.7 for the sample SBM150 and 27.9 for sample SBM250 at 150 °C.

Fluctuations such as capillary waves may not play an important role for the investigated system, which might be a consequence of the thin film preparation. It was shown in one of our previous papers[28] that TEM investigation on much thicker samples yields comparable values for the interfacial width. Fluctuations could be quenched by the influence of the smooth substrate and surface and may also not have fully developed within the annealing time. In addition, large fluctuations are damped out due to the finite film dimensions, and only those fluctuations are recorded in NR experiments, which can be seen within the lateral coher-

ence length of the incident neutrons (typically some micrometers depending on the angle of incidence).

Within the weak segregation limit (WSL) the microscopic density profile of the components is considered to vary sinusoidal in space, and the chains of the components are highly interpenetrating. It was shown by various authors that between the weak and strong segregation limits an intermediate segregation regime (ISR) between $12.5 < \chi N < 95$ can be indentified (crossover between ISR and SSL at $\chi N \approx 50$ [29]). The chains are stretched due to the coarsening of the density profile as χN is increased from the WSL.[30] The interface is relatively broad, and the junction points are not completely localized in the interfacial region. The strength of segregation expressed by χN is about 28 for sample SBM250, which means that this sample is intermediately segregated. This result puts the measured large value of interface width determined by NR in the right perspective with respect to the smaller values calculated utilizing strong segregation theory (eq 8). For sample SBM150 the strength of segregation is only about 17, which indicates that this block copolymer is almost weakly segregated. The obtained interaction paramter is much smaller as found for poly(styrene-*b*-isoprene) diblock copolymers which means that PS-*b*-PBMA is a weakly interacting system where molecular packing differences lead to differences in free volume and thermal expansion coefficients. This differences are responsible for the LCOT behavior of this system.[38] The observed large interface width and low χ parameter for the investigated system are confirming the observed partial miscibility at $M_n > 200$ kg/mol and different compositions observed by DMA.[18,19,31]

Mechanical Properties

It has already been described previously in refs 18, 19, and 32 that PS-*b*-PBMA diblock copolymers show a strong increase of tensile strength with increasing PS content. In contrast to other diblock copolymers, we find at 76% PS a maximum of tensile strength (Figure 9), which is about 40% higher than that of pure PS.[32] This synergism of tensile strength was found in the composition range between 70% and 80% PS content. The increase of the PS content to 70% leads to a tensile strength which almost approaches that of pure PS. At the transition of a mixed lamellar/hexagonal to a pure hexagonal morphology at 76% PS content the strain at break decreased, and the block copolymers become brittle.[32] With a further increase of polystyrene content up to 83% the block copolymers behave almost like polystyrene. Also, for PMMA-*b*-PBMA diblock copolymers a maximum of tensile strength was observed which exceeds the value of pure PMMA. However, in contrast to PS-*b*-PBMA diblock copolymers, the tensile strength for a sample with 77% PMMA is only about 10% higher than that of pure PMMA (Figure 9). The strain at break decreased for both systems with increasing PS contents, which was already observed for other block copolymer systems. The strain at break of PMMA-*b*-PBMA diblock copolymers is for all compositions smaller than that of PS-*b*-PBMA diblock copolymers, which is attributed to the stronger incompatibility of the components in PMMA-*b*-PBMA (Figure 10).

The reasons for the observed different tensile properties of PS-*b*-PBMA and PMMA-*b*-PBMA diblock copolymers can be discussed on the basis of the different interaction parameters χ between the components. For

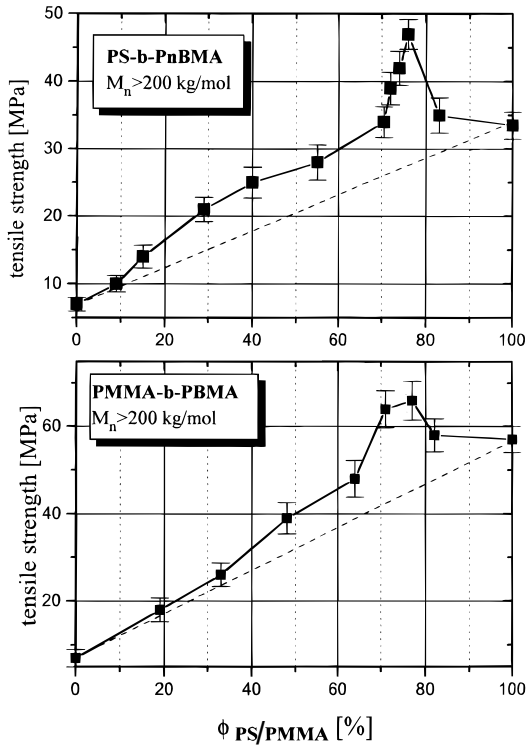

Figure 9. Dependence of tensile strength on volume fraction for PS-*b*-PnBMA and PMMA-*b*-PnBMA diblock copolymers with $M_n > 200$ kg/mol at a strain rate of $\dot{\epsilon} = 1.6 \times 10^{-4}$ s^{-1}.

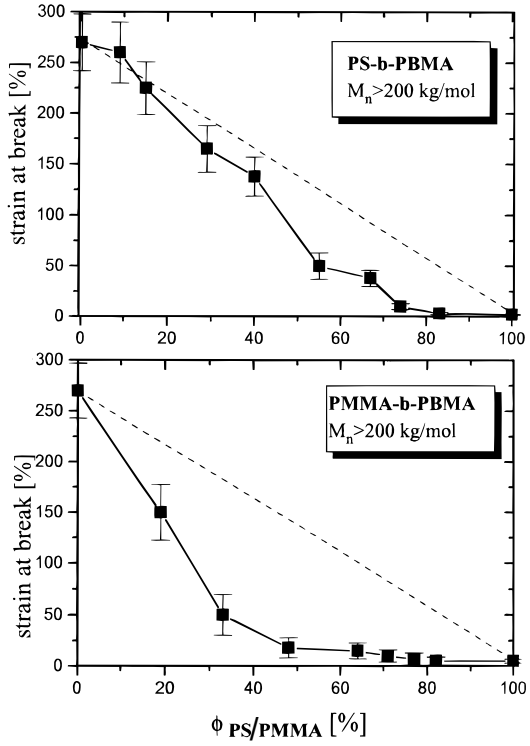

Figure 10. Dependence of strain at break on volume fraction for PS-*b*-PnBMA and PMMA-*b*-PBMA diblock copolymers with $M_n > 200$ kg/mol at a strain rate of $\dot{\epsilon} = 1.6 \times 10^{-4}$ s^{-1}.

a symmetrical dPMMA-*b*-PBMA diblock copolymer with 45.7 kg/mol, the interaction parameter was determined to $\chi_{PMMA/PBMA} = 0.062$ at $T = 140$ °C.[33] In contrast, for dPS-*b*-PBMA diblock copolymers χ was determined to 0.0133 at $T = 140$ °C by SANS, which is smaller compared to that of PMMA-*b*-PBMA diblock copolymers. However, for both systems χ is much smaller than

obtained for poly(styrene-*b*-isoprene) diblock copolymers ($\chi = 71.4/T - 0.00857$[37]). For a symmetrical PMMA-*b*-PBMA diblock copolymer with an overall molecular weight of 429 kg/mol χN is 225; which means that this sample is strongly segregated. For samples in the composition range between 70% and 80% PMMA content χN is about 120 ($M_n \approx 200$ kg/mol). We could assume that samples with asymmetrical compositions are not strongly segregated because for this compositions the value of $(\chi N)_{critical}$ increases as compared to that of symmetrical compositions. In contrast to this, PS-*b*-PBMA diblock copolymers are intermediately segregated at 120 °C where the films were annealed. (For a sample with $M_n = 278$ kg/mol and 50% PS content one obtains $\chi N_{120°C} = 29.5$). It should be kept in mind that deuteration also changes the thermodynamics slightly if we compare deuterated and nondeuterated samples. This effect is believed to be relatively small, and we assume that it is not important for our discussions. A smaller interface width was observed for dPMMA-*b*-PBMA diblock copolymers (e.g., about 3.5 nm at $T = 140$ °C determined for a sample with $M_n = 45.7$ kg/mol and 43% PMMA[34]). A comparable diblock copolymer of dPS-*b*-PBMA has a interface width of 7.7 nm at $T = 140$ °C.[28] The difference is due to larger interaction parameter between the blocks in PMMA-*b*-PBMA diblock copolymers.

Bühler et al.[34] have shown that a broadened interface in block copolymers can improve the strength which is in accordance with our results. Usually one assumes that the interfacial region contains a larger amount of defects resulting in a low interfacial strength. For diblock copolymers chain ends are localized predominantly in the middle of the phases, and the chemically coupled chains in the interfacial region can enhance the strength as compared to homopolymer blends. Bühler and Gronski[35] have shown for block copolymers that an increasing interfacial width leads to a decreasing interfacial energy. This decrease of interfacial energy is associated with a decreasing stress concentration at the interface which is responsible for the improvement of tensile strength. Whereas in the WSL the chains of the components are highly interpenetrating, in the ISR the chains are stretched which also could have a pronounced influence on tensile properties. It was shown elsewhere[32] that the Young's modulus of PS-*b*-PBMA diblock copolymers exceeds that of pure homopolymers at a PS content of 76%, which was not observed for PMMA-*b*-PBMA diblock copolymers. The reason for this observation could be attributed to the stretched chain conformation combined with the observed broadened interface in PS-*b*-PBMA diblock copolymers.

Conclusions

The phase behavior of dPS-*b*-PBMA diblock copolymers was investigated by SANS, NR, and rheology. It was found that for a symmetrical partially deuterated sample with 90 kg/mol the strong discontinuity of $I(q^*)$, Δq, and G' at 155 °C can be clearly attributed to the disorder−order transition (LCOT) at this temperature. The interaction parameter increases with increasing temperature, indicating a LCOT system where the entropic contribution to χ is larger than the enthalpic contribution. The quite small χ leads to weak and intermediate segregation at much higher molecular weights where the interfacial width determined by NR is quite large as compared to the case of PS-*b*-PI diblock copolymers.

Using those data, we are able to correlate the phase behavior and tensile properties of block copolymers. It was shown that a decrease of miscibility and interface width in the case of PBMA-*b*-PMMA leads to less pronounced tensile properties. The relatively large miscibility (small interaction parameter) of PS-*b*-PBMA block copolymers combined with a large interfacial width and asymmetrical phase compositions provide the basis for synergistic effects on tensile properties of weakly segregated block copolymers.

Acknowledgment. R. Weidisch acknowledges postdoctoral support from Deutsche Forschungsgemeinschaft (DFG). We also acknowledge the help of Dr. P. Staron (GKSS Geesthacht) and M. Pannek (GKSS Geesthacht) during the SANS and NR measurements and the data processing procedures.

References and Notes

(1) Holden, G. In *Thermoplastic Elastomers*; Legge, N. R., Holden, G., Schroeder, H. E., Eds.; Hanser: Muinch, 1987; pp 481−506.
(2) Haward, R. N.; Young, R. J. *The Physics of Glassy Polymers*; Chapman & Hall: London, 1997.
(3) Hashimoto, T.; Yamasaki, K.; Koizumi, S.; Hasegawa, H. *Macromolecules* **1994**, *26*, 1562.
(4) Thomas, E. L.; Alward, D. B.; Kinning, D. J.; Martin, D. C.; Handlin, D. L.; Fetters, L. J. *Macromolecules* **1987**, *20*, 1651.
(5) Winey, K. I.; Gobran, D. A.; Xu, Z.; Fetters, L. J.; Thomas, E. L. *Macromolecules* **1994**, 27, 2392.
(6) Spontak, R. J.; Smith, S. D.; Ashraf, A. *Macromolecules* **1993**, *26*, 2233.
(7) Hamley, I. W.; Koppi, K. A.; Rosedale, J. H.; Bates, F. S.; Almdal, K.; Mortensen, K. *Macromolecules* **1993**, *26*, 5959.
(8) Hadjuk, D. A.; Harper, P. E.; Gruner, S. M.; Honeker, C. C.; Kim, G.; Thomas, E. L.; Fetters, L. J. *Macromolecules* **1994**, *27*, 4063.
(9) Förster, S.; Khanpur, A. K.; Zhao, J.; Bates, F. S.; Hamley, I. W.; Ryan, A. J.; Bras, W. *Macromolecules* **1994**, *27*, 6922.
(10) Russell, T. P.; Karis, T. E.; Gallot, Y.; Mayes, A. M. *Nature* **1994**, *368*, 729.
(11) Karis, T. E.; Russell, T. P.; Gallot, Y.; Mayes, A. M. *Macromolecules* **1995**, *28*, 1129.
(12) Pollard, M.; Russell, T. P.; Ruzette, A. V.; Mayes, A. M.; Gollot, Y. *Macromolecules* **1998**, 31, 6493.
(13) Stokmayer, W. H.; Stanley, H. E. *J. Chem. Phys.* **1950,** *18*, 153.
(14) Benoit, H.; Wu, W.; Benmouna, M.; Moser, B.; Bauer, B.; Lapp, A. *Macromolecules* **1985**, *18*, 986.
(15) Fuduka, T.; Inagaki, H. *Pure Appl. Chem.* **1983,** *55*, 1541.
(16) Schubert, D. W.; Abetz, V.; Stamm, M.; Hack, T.; Siol, W. *Macromolecules* **1995**, *28*, 8, 2519.
(17) Arnold, M.; Hofmann, S.; Weidisch, R.; Neubauer, A.; Poser, S.; Michler, G. H. *Macromol. Chem. Phys.* **1998**, *199*, 31.
(18) Weidisch, R.; Michler, G. H.; Arnold, M.; Hofmann, S.; Stamm, M.; Jérôme, R. *Macromolecules* **1997**, *30*, 8078.
(19) Weidisch, R.; Michler, G. H.; Fischer, H.; Hofmann, S.; Arnold, M.; Stamm, M. *Polymer* **1999**, *40*, 1191.
(20) Schubert, D. W. *Polym. Bull.* **1997**, *38*, 177.
(21) Rosedale, J. H.; Bates, F. S.; Almdal, K.; Mortensen, K.; Wignall, G. *Macromolecules* **1995**, *18*, 1429.
(22) Foster, M. D.; Sikka, M.; Singh, N.; Bates, F. S.; Satija, S. K.; Majkrzak, C. F. *J. Chem. Phys.* **1992**, *96*, 8605.
(23) Leibler, L. *Macromolecules* **1980**, *13*, 1302.
(24) Russell, T. P.; Hjelm, R. P.; Seeger, P. A. *Macromolecules* **1990**, *23*, 890.
(25) Brasovskii, S. A. *Sov. Phys. JETP* **1975**, *41*, 85.
(26) Stamm, M.; Schubert, D. W. *Annu. Rev. Mater. Sci.* **1995**, *25*, 325.
(27) Binder, K. *Adv. Polym. Sci.* **1994**, *112*, 115.
(28) Schubert, D. W.; Weidisch, R.; Stamm, M.; Michler, G. H. *Macromolecules* **1998**, *31*, 3743.
(29) Matsen, M. W.; Bates, F. *Macromolecules* **1996**, *29*, 1091.
(30) Melenkevitz, J.; Muthukumar, M. *Macromolecules* **1991**, *24*, 4199.
(31) Weidisch, R.; Michler, G. H.; Arnold, M. *Polymer*, in press.

(32) Weidisch, R.; Stamm, M.; Fischer, H.; Michler, G. H.; Jerome, R. *Macromolecules* **1999**, *32*, 742.
(33) Scherble, J.; Stark, B.; Stühn, B.; Kressler, J.; Schubert, D. W.; Budde, H.; Höring, S.; Simon, P.; Stamm, M. *Macromolecules* **1999**, *32*, 1859.
(34) Bühler, F. Doctoral Dissertation, Freiburg, 1986.
(35) Bühler, F.; Gronski, W. *Makromol. Chem.* **1987**, *188*, 2995.
(36) Semenov, A. N. *Macromolecules* **1993**, *26*, 6617.
(37) Khandpur, A. K.; Förster, S.; Bates, F. S.; Hamley, I. W.; Ryan, A. J.; Bras, W.; Almdal, K.; Mortensen, K. *Macromolecules* **1995**, *26*, 8796.
(38) Ruzette, A.; Banerjee, P.; Mayes, A. M.; Pollard, M.; Russell, T. P.; Jerome, R.; Slawecki, T.; Hjelm, R.; Thiyagarajan, P. *Macromolecules* **1998**, *31*, 8509.

MA981748T